

# HIGGS BOSON SEARCH AT PHOTON COLLIDER FOR $M_H = 140 - 190$ GEV.

I.F.Ginzburg, I.P.Ivanov\*

Institute of Mathematics, Novosibirsk, e-mail: ginzburg@math.nsc.ru

## Abstract

A Higgs boson within the mass range  $M_H = 140 - 190$  GeV can be discovered at a photon collider in the reaction  $\gamma\gamma \rightarrow WW$  (with real or virtual  $W$ ) with the luminosity integral about  $1 \text{ fb}^{-1}$ . The reasonable resolution in the effective mass of the  $WW$  system is required.

## Preliminary remarks.

A discovery of the Higgs boson is one of the main goals for the next generation of colliders.

If the Higgs boson mass  $M_H$  is larger than  $2M_Z$ , it can be discovered at LHC, photon colliders [1] or  $e^+e^-$  linear colliders [2] via the sizable decay mode  $H \rightarrow ZZ$ . For all types of collisions a background to this decay mode is rather small. If  $M_H < 145$  GeV the Higgs boson can be discovered at  $e^+e^-$  linear colliders or photon colliders via the dominant decay mode  $H \rightarrow b\bar{b}$  and at LHC – via the decay mode  $H \rightarrow \gamma\gamma$ .

The mass range  $M_H = 140 - 190$  GeV is the most difficult one for the Higgs boson discovery. In this mass range the decay mode  $H \rightarrow W^+W^-$  with real or virtual  $W$ 's ( $W^* \rightarrow q\bar{q}, e\bar{\nu}, \dots$ ) is dominant, branching ratios of other decay modes decrease rapidly and their using for the Higgs boson discovery is very difficult. The use of the  $H \rightarrow W^+W^-$  decay at  $e^+e^-$  collider is also difficult due to a strong nonresonant  $W^+W^-$  background. (See review [3] and references therein for more details). As for observation of such Higgs boson at photon collider, it was noted that "the  $WW$  final state will be a difficult one to use for doing Higgs physics" [4]. The opportunity to see Higgs boson with  $M_H \sim 2M_W$  via  $WW$  mode at photon collider was noted in ref. [6], where nonrealistic photon spectrum was used and the interference effects were neglected.

In this letter, we show that the Higgs boson with the mass  $M_H = 140 - 190$  GeV can be discovered at the photon collider via the  $H \rightarrow W^+W^-$  decay mode.

To this end we consider both resonant  $\gamma\gamma \rightarrow H \rightarrow W^+W^-$  and nonresonant QED contributions into this process:

$$d\sigma \propto |\mathcal{M}|^2 \equiv |\mathcal{M}^0|^2 + 2\text{Re}(\mathcal{M}^{0*}\mathcal{M}^H) + |\mathcal{M}^H|^2. \quad (1)$$

Here  $|\mathcal{M}^0|^2$  stands for the background QED process  $\gamma\gamma \rightarrow W^+W^-$ ,  $|\mathcal{M}^H|^2$  is the contribution of  $\gamma\gamma \rightarrow H \rightarrow W^+W^-$  and  $2\text{Re}(\mathcal{M}^{0*}\mathcal{M}^H)$  describes the interference effect of these two mechanism.

---

\*Novosibirsk State University

The interference contribution is negligible both at high enough masses of Higgs [5] and far below the nominal threshold (at  $M_{WW} < 2M_W$ ). The interference was neglected in calculations of [6] for entire mass region. In fact, for  $M_H = 200 - 300$  GeV the interference appeared to be not small [7]. Its magnitude increases with decrease in  $M_H$ . The range of  $M_{WW}$  where the deviation from the nonresonant background is noticeable, coincides with the Higgs boson width  $\Gamma_H$ , therefore this range also decreases with decrease in  $M_H$ . After averaging over a reasonable interval of  $M_{WW}$  the effect was still noticeable providing an additional way to study the Higgs boson coupling with  $W$  bosons [7].

We use these considerations as a starting point following a proposal [8].

### The $WW$ production cross section at $140 < M_{WW} < 190$ GeV.

We consider initial photon state with total helicity zero (helicities of colliding photons  $\lambda_1 = \lambda_2 = \pm 1$ ). Only a photon state with such quantum numbers can produce the Higgs boson. Helicity amplitudes for the nonresonant process (in the Born approximation) for such initial state are presented in ref. [10]. In this case the helicities  $\lambda$  of produced  $W$  bosons coincide. One has (the subscript corresponds to helicity of produced  $W$ ,  $\Lambda$  is the product of the photon and  $W$  helicities):

$$\mathcal{M}_0^0 = -\frac{2\pi\alpha s x}{p_\perp^2 + M_W^2}; \quad \mathcal{M}_{\pm 1}^0 = \frac{\pi\alpha s}{p_\perp^2 + M_W^2} (2\Lambda\sqrt{1-x} + 2-x) \quad \left(x = \frac{4M_W^2}{s}\right). \quad (2)$$

The amplitude  $\mathcal{M}^H$  is written in the standard form via the well known amplitude of Higgs boson two photon decay [9].

In practice we deal with the production of four fermions in the final state produced via intermediate  $W$  boson state. The distribution in invariant masses for such final state has a maximum at  $M_W$  with the width  $\Gamma_W$  and long tails away from the maximum. It can be described by the well known Breit–Wigner spectral density for the  $W$  boson. One can view this as the production of  $W^*$  — a virtual  $W$  boson with the mass not equal to  $M_W$ . Because of this, the cross section does not vanish below the nominal threshold  $M_{WW}^{thr} = 2M_W$ . The most important effect comes from the corresponding modification in the final phase space [5]. It can be described via replacement of the relative velocity of  $W$  bosons in the center of mass frame

$$\beta = \frac{1}{s} \sqrt{(s - s_1 - s_2)^2 - 4s_1 s_2}$$

by its convolution with above spectral density for the  $W$  boson  $\varrho(M^2)$ :

$$\beta \rightarrow \tilde{\beta} = \int ds_1 ds_2 \varrho(s_1) \varrho(s_2) \beta(s, s_1, s_2) \theta(s_1) \theta(s_2) \theta(\sqrt{s} - \sqrt{s_1} - \sqrt{s_2}).$$

Close to the threshold the  $\gamma\gamma \rightarrow W^+W^-$  cross section for stable  $W$  bosons can be approximated as:

$$\sigma \propto |\mathcal{M}|_{s=4M_W^2}^2 \beta,$$

We do not have explicit formulas for the background process below the threshold. Therefore, we restrict ourselves to the approximation where helicity amplitudes are calculated at the nominal threshold  $2M_W$  neglecting the effect of the finite width. Finally, we approximate cross section near the threshold by equation

$$\sigma \propto |\mathcal{M}|_{s=4M_W^2}^2 \tilde{\beta},$$

The accuracy of this approximation can be checked by comparing exact calculation for the Higgs boson width  $\Gamma_{H \rightarrow W^+W^-}^{prec}$  (based on ref. [11]) with our approximation. Let us denote the Higgs boson width obtained in the framework of our approximation as  $\Gamma_{H \rightarrow W^+W^-}^{phas}$ . We find then that the ratio  $\Gamma_{H \rightarrow W^+W^-}^{prec} / \Gamma_{H \rightarrow W^+W^-}^{phas}$  varies from 1.2 for  $M_H = 160$  GeV to 1.6 for  $M_H = 140$  GeV. Note, that the Higgs boson width itself decreases by a factor of 20 for  $M_H = 140$  GeV in comparison with its value at  $M_H = 160$  GeV, so one can conclude that our approximation works well.

Let us now describe the results of the calculation. In our estimates we neglected angular dependence of the cross sections (since we are working in the threshold region) and integrated over production angle in the center of mass frame within the range  $20^\circ < \theta < 160^\circ$ . This represents 94% of the total solid angle.

In Fig. 1 we show  $\gamma\gamma \rightarrow W^+W^-$  cross section for various  $M_H$  as a function of the invariant mass  $M_{WW}$  of the  $W^+W^-$  pair for the initial state with total helicity zero. For  $M_H \geq 180$  GeV the two-peak behavior observed in [7] is seen clearly. The interference term in eq. (1) is large for such Higgs boson masses. The height of the peak grows with decrease in  $M_H$  but its width ( $\approx \Gamma_H$ ) becomes smaller and smaller.

With subsequent decrease in  $M_H$ , the background QED process is suppressed by the phase space and the interference also becomes small in comparison with the Higgs boson contribution.

### The “experimental” cross sections.

After averaging over initial energy distribution of the photons, the Higgs boson signal decreases and seems to be hardly observable. To circumvent this problem, the observation of  $W$  bosons in the final state is mandatory (perhaps, via quark jets). In order to account for a finite resolution in  $M_{WW}$ , we consider a “smeared” cross section, similar to [7]:

$$\frac{d\sigma}{dM_{WW}^{meas}} = \int \frac{dM_{WW}}{\sqrt{2\pi} d} \exp \left[ -\frac{(M_{WW}^{meas} - M_{WW})^2}{2d^2} \right] \frac{d\sigma}{dM_{WW}} \quad (3)$$

The results for  $d = 5$  GeV are presented below.

Let us stress that we do not perform any convolution with initial photon spectra. It is because of the fact that the real form of these effective spectra strongly depends on the details of the conversion design. Note also, that it can not be obtained by a simple convolution of individual spectra [1]. Real energy distribution of colliding photons should be measured for every energy of collider<sup>1</sup>. We have in mind “monochromatic” variant of the photon collider with the effective width of the  $\gamma\gamma$  energy distribution  $\sim 15\%$  [1, 2].

The results of this calculation are shown in Fig. 2 (above the nominal threshold), in Fig. 3 (below the nominal threshold) and in the Table.

In view of a very high degree of photon polarization expected at photon colliders, we present the Figures for completely polarized photon beams:  $\langle \lambda_1 \rangle = \langle \lambda_2 \rangle = \pm 1$ . Higgs boson signal deteriorates when  $\langle \lambda_1 \rangle \langle \lambda_2 \rangle$  decreases. Some result for  $\langle \lambda_i \rangle \neq 1$  are presented in the Table for “realistic” mean helicities of the photons [1, 2].

Above the nominal threshold the curves in Fig. 2 exhibit a characteristic shape. A deviation from the QED background is very sensitive to the presence of the Higgs boson. Therefore, such behavior of the experimental curve can be considered as an evidence for

---

<sup>1</sup> The effect of averaging over initial photon spectrum without reconstruction of  $M_{WW}$  can be simulated by using  $d \approx 15$  GeV in eq. (3) (cf. [1],[2]).

| Higgs boson mass<br>$M_H$ , GeV | Characteristic<br>$M_{WW}$ , GeV | $\langle \lambda \rangle$ | $\sigma^{bkgd}$ , pb | $\sigma^{tot}$ , pb | $\frac{\sigma^{tot} - \sigma^{bkgd}}{\sigma^{bkgd}}$ |
|---------------------------------|----------------------------------|---------------------------|----------------------|---------------------|--|
| 140                             | 140                              | 1.0                       | 0.11                 | 0.98                | 8.0  |
|                                 |                                  | 0.9                       | 0.17                 | 0.96                | 4.6  |
| 150                             | 150                              | 1.0                       | 0.42                 | 2.10                | 4.0  |
|                                 |                                  | 0.9                       | 0.60                 | 2.13                | 2.6  |
| 160                             | 159.7                            | 1.0                       | 3.65                 | 6.81                | 87%  |
|                                 |                                  | 0.9                       | 4.86                 | 7.74                | 59%  |
| 170                             | 169.3                            | 1.0                       | 12.6                 | 15.5                | 23%  |
|                                 |                                  | 0.9                       | 16.0                 | 18.5                | 16%  |
| 180                             | 178.5                            | 1.0                       | 21.8                 | 23.7                | 8.7%   |
|                                 |                                  | 0.9                       | 25.3                 | 27.0                | 6.7%   |
| 190                             | 185                              | 1.0                       | 26.0                 | 27.0                | 3.8%   |
|                                 |                                  | 0.9                       | 29.9                 | 30.8                | 3.0%   |
|                                 | 200                              | 1.0                       | 37.3                 | 36.5                | -2.1%  |
|                                 |                                  | 0.9                       | 40.2                 | 39.4                | -2.0%  |

Table 1:  $\gamma\gamma \rightarrow W^+W^-$  cross sections for various  $M_H$  and  $\langle \lambda \rangle$

the existence of the Higgs boson in this mass region. Here the background QED cross section varies from 3.6 pb for  $M_{WW} = 160$  GeV to 30 pb for  $M_{WW} = 190$  GeV. The Higgs boson production cross section adds another 3 pb for  $M_H = 160$  GeV (87%). For  $M_H = 190$  GeV an interference term in eq. (1) delivers 1.8 pb (6%) to the total cross section.

Below the threshold Higgs boson is observed even more clearly (Fig. 3). The total cross section is about 1 pb in the whole region. It is larger than the cross section for the background process by almost a factor of 2 for  $M_H = 160$  GeV and by a factor of 9 for  $M_H = 140$  GeV. This result is in qualitative agreement with that in ref. [6].

This behavior is not surprising. The total Higgs boson production cross section averaged over the range of  $M_{WW}$  larger than the total width of the Higgs boson is equal to  $\sigma_{\gamma\gamma \rightarrow H} = 4\pi^2\Gamma_{\gamma\gamma}/M_H^3$ . The Higgs boson width drops out in this result. Roughly speaking, the cross section is almost independent of  $M_H$  in the considered mass range. At the same time, down to  $M_H = 145$  GeV the  $W^+W^-$  decay mode still remains dominant. On the other hand, the QED background decreases fast with decrease in  $M_{WW}$  in the considered mass range. For this reason the two peak behavior, observed for  $M_H > 180$  GeV, changes to a single resonance peak near and below the threshold and the Higgs boson signal becomes dominant in this region.

As was discussed above, more precise calculation of the Higgs boson width would enhance the effect by a factor  $\sim 1.6$  for  $M_H = 140$  GeV. We expect that the signal-to-background ratio will be close to the one calculated in this paper.

### Discussion. Final remarks.

We conclude that the Higgs boson with the mass  $M_H = 140 - 190$  GeV can be observed and studied in the process  $\gamma\gamma \rightarrow W^+W^-$  at future  $\gamma\gamma$  colliders by measuring the invariant mass of produced  $W^+W^-$  system with reasonable resolution. A luminosity

integral required for this observation is  $\sim 1 \text{ fb}^{-1}$ . This value seems to be sufficient even accounting for corrections due to detection efficiency etc., and the electromagnetic 4 jet production<sup>2</sup>.

Moreover, we found that for  $M_H \leq 160 \text{ GeV}$  the effect of the Higgs boson is still seen after being smeared over 15 GeV. This means that the signal of the Higgs boson lighter than 160 GeV can be observed even in the total  $\gamma\gamma \rightarrow W^+W^-$  cross section without restrictions on the  $W^+W^-$  invariant mass.

Additionally, if the Higgs boson mass is near 140 GeV, one can hope to observe Higgs boson decays into  $b\bar{b}$  and  $W^+W^-$ . It provides an opportunity to compare the Higgs boson coupling to quarks and to gauge bosons and in this way to test the Higgs boson origin of particle masses.

Last, similar calculation can be easily repeated for  $\gamma\gamma \rightarrow H \rightarrow ZZ$  process below its nominal threshold (the nonresonant background is negligible here). The corresponding cross sections are  $\sim 50 \text{ fb}$ . Therefore, provided the luminosity integral  $\sim 10 \text{ fb}^{-1}$ , one can also observe a Higgs boson in  $ZZ$  decay mode in the whole region of  $M_H$  considered here. The comparison of Higgs boson couplings with different gauge bosons will be essential test of SM concerning Higgs mechanism of the mass origin.

Our analyses at this point should be considered as an estimate of the effect. We are sure that our estimates give correct order of magnitude prediction for the signal to background ratio. However, more studies are required to arrive at absolute predictions. At the first stage of such studies Born approximations for all quantities should be improved by taking into account relatively large corrections due to the finite  $W$  width in  $\gamma\gamma \rightarrow H$  amplitude [12].

This work is supported by grants INTAS – 93–1180 ext and RFBR – 96–02–19114. We are grateful to A.E. Bondar, J.F. Gunion, K.V. Melnikov, V.G. Serbo and V.I. Telnov for discussions.

## References

- [1] I.F. Ginzburg, G.L. Kotkin, V.G. Serbo and V.I. Telnov, Sov. ZhETF Pis'ma. 34 (1981) 514; Nucl. Instr. and Methods in Physics Research (NIMR) 205 (1983) 47; I.F. Ginzburg, G.L. Kotkin, S.L. Panfil, V.G. Serbo and V.I. Telnov, NIMR 219 (1983) 5.
- [2] Zeroth-order Design Report for the NLC, SLAC Report 474 (1996); TESLA, SBLC Conceptual Design Report, DESY (1997) To be published.
- [3] J.F. Gunion, L. Poggiolli and R. van Kooten, Higgs Boson Discovery and Properties, hep-ph/9703330 (1997).
- [4] D.L. Borden, D.A. Bauer and D.O. Caldwell, Phys. Rev. **D48** (1993) 4018.
- [5] I.F. Ginzburg, G.L. Kotkin, S.L. Panfil and V.G. Serbo, Nucl. Phys. **B228** (1983) 285.

---

<sup>2</sup> The cross section is saturated by events with effective mass of decay products of one  $W$  boson lying within the resonance peak. Above the threshold the same is valid for the other  $W$  boson, below the threshold the corresponding effective mass is below the resonance peak.

- [6] J.F. Gunion and H.E. Haber, Phys. Rev. **D48** (1993) 5109.
- [7] D.A. Morris, T.N. Truong and D. Zappala, Phys. Lett. **B323** (1994) 421.
- [8] I.F. Ginzburg, Proc. Workshop “ $e^+e^-$  Collisions at TeV Energies. The Physics Potential”. Part D. DESY 96–123D (1996) 463–472.
- [9] A.I. Vainshtein, M.B. Voloshin, V.I. Zakharov, and M.A. Shifman, Sov. J. Nucl. Phys. **30** (1979) 711.
- [10] G. Belanger and F. Boudjema, Phys. Lett. **B288** (1992) 210.
- [11] E. Gross, B. Kniehl and G. Wolf, Z. Phys. **C63** (1994) 417.
- [12] K. Melnikov, M. Spira and O.I. Yakovlev, Z. Phys. **C64** (1994) 401.

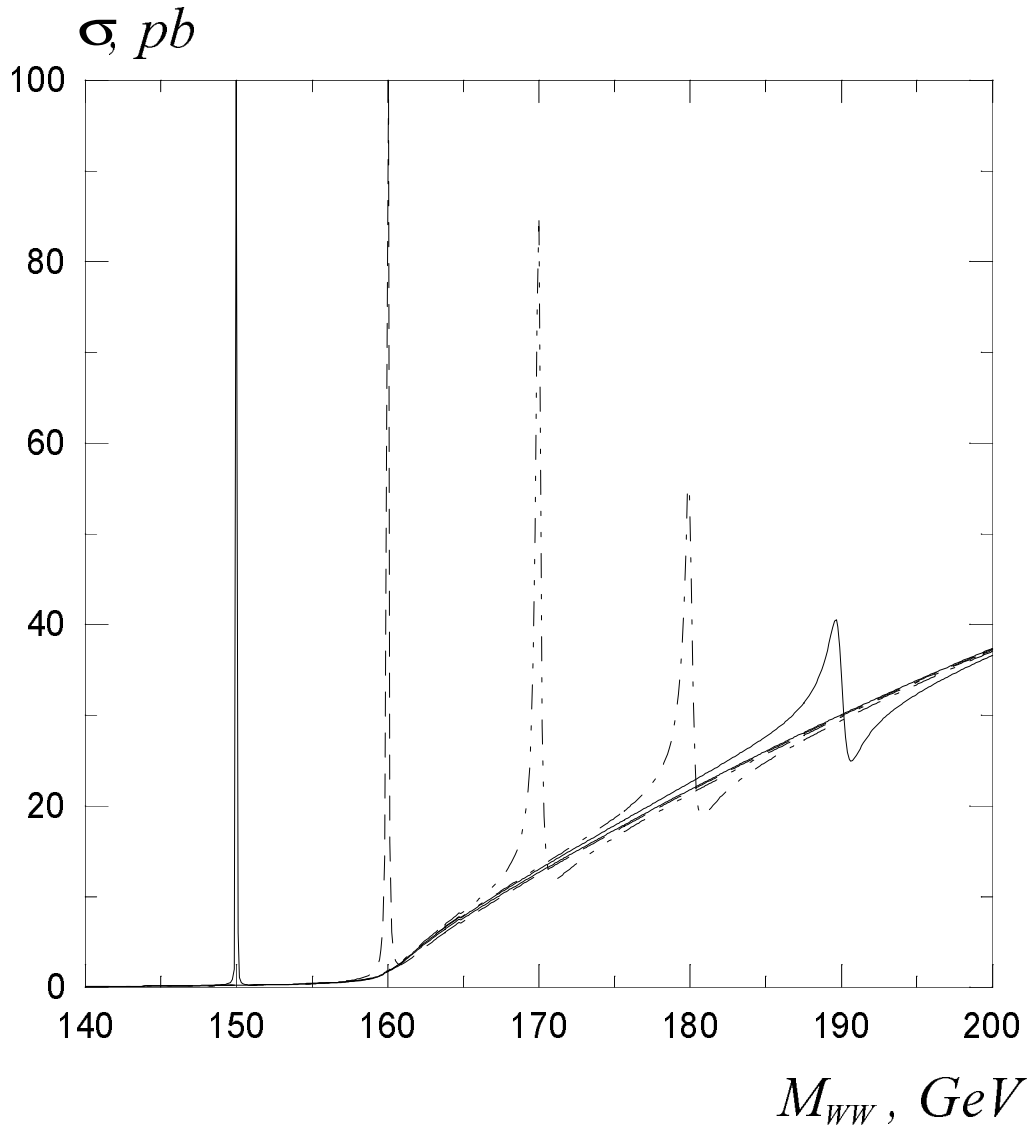


Fig.1. The  $\Upsilon\Upsilon \Rightarrow WW$  cross sections for different  $M_H$ .

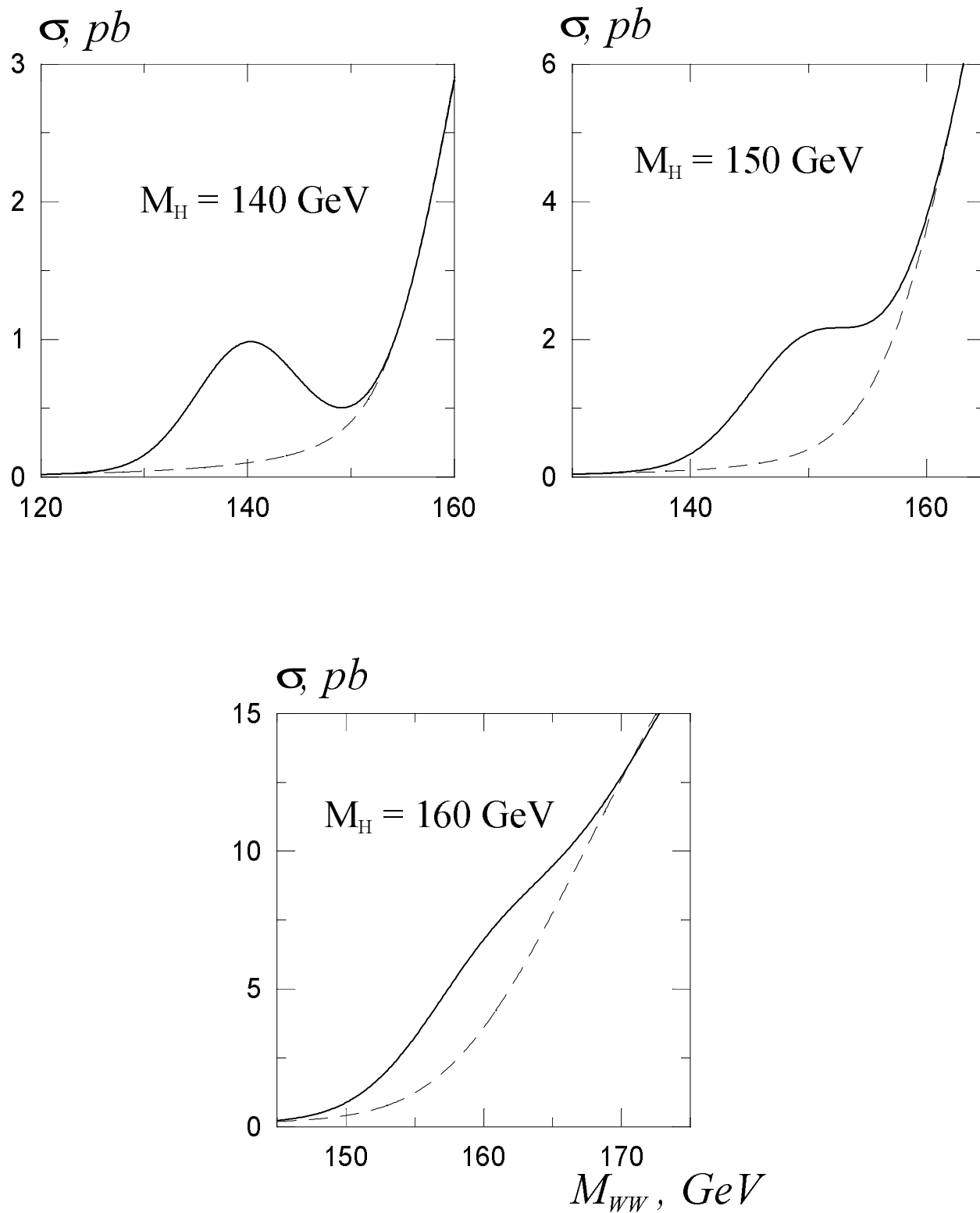


Fig.2. Smeared cross sections below the threshold.  
 Dashed lines - nonresonant background.



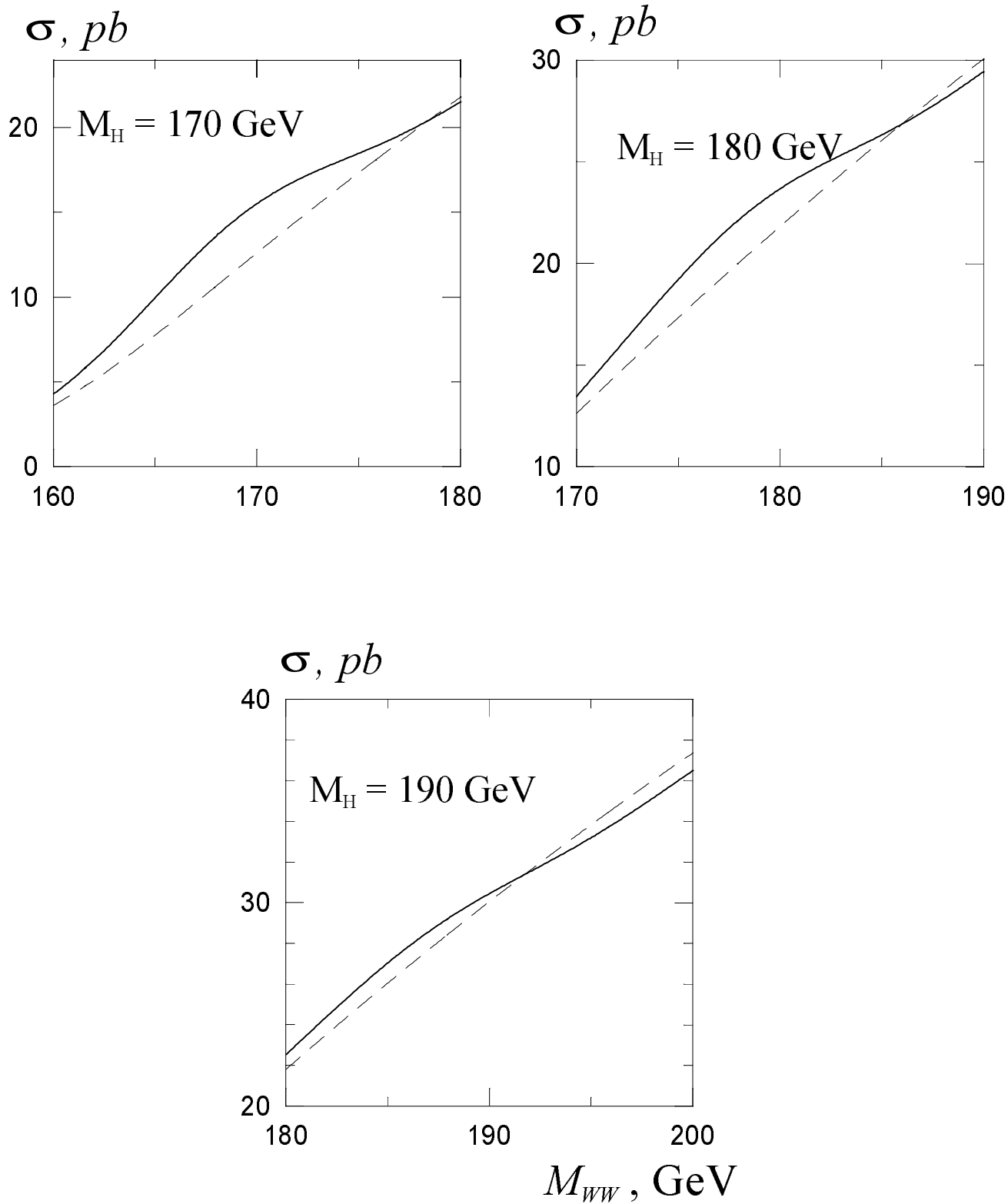


Fig.3. Smeared cross sections above the threshold.  
Dashed lines - nonresonant background.